



Supplementary Materials for

Structural basis of eIF2B-catalyzed GDP exchange and phosphoregulation by the integrated stress response

Lillian R. Kenner^{1,†}, Aditya A. Anand^{1,2,†}, Henry C. Nguyen¹, Alexander G. Myasnikov¹, Lea A. McGeever^{1,2}, Carolin J. Klose^{1,2}, Jordan C. Tsai^{1,2}, Lakshmi E. Miller-Vedam^{1,2,3}, Peter Walter^{1,2,*}, Adam Frost^{1,3,*}

Correspondence to: peter@walterlab.ucsf.edu; adam.frost@ucsf.edu

This PDF file includes:

Materials and Methods
Supplementary Text
Figs. S1 to S8
Tables S1 to S3
Captions for Movies S1

Other Supplementary Materials for this manuscript include the following:

Movies S1

Materials and Methods

Purification of decameric eIF2B($\alpha\beta\gamma\delta\epsilon$)₂

As previously described (17), pJT066, pJT073, and pJT074 were co-transformed into One Shot BL21 Star (DE3) chemically competent *E. coli* cells (Invitrogen) and grown in Luria broth containing ampicillin, kanamycin, and chloramphenicol at 37°C on an orbital shaker. When the culture reached an OD600 of ~0.6, the temperature was reduced to 16°C, and the culture was induced with 0.8 mM IPTG (Gold Biotechnology) and grown for 16 hours. Cells were harvested and lysed with an EmulsiFlex-C3 (Avestin) in a buffer containing 20 mM HEPES-KOH, pH 7.5, 250 mM KCl, 1 mM tris(2-carboxyethyl)phosphine (TCEP), 5 mM MgCl₂, 15 mM imidazole, and complete EDTA-free protease inhibitor cocktail (Roche). The lysate was clarified at 30,000g for 20 min at 4°C. Subsequent purification steps were conducted on the ÄKTA Pure (GE Healthcare) system at 4°C. The clarified lysate was loaded onto a HisTrap HP 5 ml, washed in binding buffer (20 mM HEPES-KOH, pH 7.5, 200 mM KCl, 1 mM TCEP, 5 mM MgCl₂, and 15 mM imidazole), and eluted with a linear gradient (75 ml) of 15 mM to 300 mM imidazole in the same buffer. The eIF2B fraction eluted from the HisTrap column at 80 mM imidazole. The eIF2B fraction was collected and loaded onto a 20 ml Mono Q HR16/10 column (GE Healthcare), washed in Buffer A (20 mM HEPES-KOH, pH 7.5, 200 mM KCl, 1 mM TCEP, and 5 mM MgCl₂) and eluted with a linear gradient (200 ml) of 200 mM to 500 mM KCl in the same buffer. The eIF2B fraction eluted off the Mono Q column at a conductivity of 46 mS/cm (corresponding to 390 mM KCl). Fractions were collected, concentrated with an Amicon Ultra-15 concentrator (EMD Millipore) with a 100,000-dalton molecular weight cutoff, and loaded onto a Superdex 200 10/300 GL column (GE Healthcare) equilibrated with Buffer A. A typical preparation yielded approximately 0.5 mg of eIF2B($\alpha\beta\gamma\delta\epsilon$)₂ from a 1-liter culture.

Purification of heterotrimeric human eIF2

Human eIF2 was prepared from an established recombinant *S. cerevisiae* expression protocol (19). In brief, the yeast strain GP6452 (gift from the Pavitt lab, University of Manchester) containing yeast expression plasmids for human eIF2 subunits and a deletion of GCN2 encoding the only eIF2 kinase in yeast, was grown to saturation in synthetic complete media (Sunrise Science Products) with auxotrophic markers (-Trp, -Leu, -Ura) in 2% dextrose. The β and α subunits of eIF2 were tagged with His6 and FLAG epitopes, respectively. A 12-liter yeast culture was grown in rich expression media containing yeast extract, peptone, 2% galactose, and 0.2% dextrose. Cells were harvested and resuspended in lysis buffer [100 mM Tris, pH 8.5, 300 mM KCl, 5 mM MgCl₂, 0.1% NP-40, 5 mM imidazole, 10% glycerol (Thermo Fisher Scientific), 2 mM DTT, 1× protease inhibitor cocktail (Sigma Aldrich #11836170001), 1 μ g/ml each aprotinin (Sigma Aldrich), leupeptin (Sigma Aldrich), pepstatin A (Sigma Aldrich)]. Cells were lysed in liquid nitrogen using a steel blender. The lysate was centrifuged at 10,000g for 1 hour at 4°C. Subsequent purification steps were conducted on the ÄKTA Pure (GE Healthcare) system at 4°C. Lysate was applied to a 5-ml HisTrap Crude column (Thermo Fisher Scientific) equilibrated in buffer (100 mM HEPES, pH 7.5, 100 mM KCl, 5 mM MgCl₂, 0.1% NP-40, 5% glycerol, 1 mM dithiothreitol, 0.5× protease inhibitor cocktail, 1 μ g/ml each aprotinin, leupeptin, pepstatin A). eIF2 bound to the column, was washed with equilibration buffer and eluted using a 50 ml linear gradient of 5 mM to 500 mM imidazole. Eluted eIF2 was incubated with FLAG M2 magnetic affinity beads, washed with FLAG wash buffer (100 mM HEPES, pH 7.5, 100 mM KCl, 5 mM MgCl₂, 0.1% NP-40, 5% glycerol, 1 mM TCEP, 1× protease inhibitor cocktail, 1

μg/ml each aprotinin, leupeptin, pepstatin A) and eluted with FLAG elution buffer [identical to FLAG wash buffer but also containing 3× FLAG peptide (100 μg/ml, Sigma Aldrich)]. Concentration of purified protein was measured by BCA assay (Thermo Fisher Scientific # PI23225); protein was flash-frozen in liquid nitrogen and stored in elution buffer at −80° C. A typical preparation yielded 1 mg of eIF2 from a 12-liter culture.

Purification of human eIF2α

Human eIF2α was *E. coli* codon-optimized, synthesized and cloned into a pUC57 vector by GenScript Inc. PCR-amplified dsDNA fragments containing the eIF2α sequence were cloned into a pET28a vector using an In-Fusion HD Cloning Kit (Takara Bio), resulting in the kanamycin-resistant expression plasmid, pAA007. pAA007 was co-transformed into One Shot BL21 Star (DE3) chemically competent *E. coli* cells (Invitrogen), along with the tetracycline-inducible, chloramphenicol-resistant plasmid, pG-Tf2, containing the chaperones groES, groEL, and tig (Takara Bio). Transformed cells were grown in Luria broth containing kanamycin and chloramphenicol at 37°C on an orbital shaker.

When the culture reached an OD600 of ~0.2, 1ng/mL tetracycline was added to induce expression of chaperones. At an OD600 of ~0.8, the temperature was reduced to 16°C, eIF2α expression was induced with 1 mM IPTG (Gold Biotechnology) and the culture was grown for 16 hours. Cells were harvested and lysed with an EmulsiFlex-C3 (Avestin) in a buffer containing 100 mM HEPES-KOH, pH 7.5, 300 mM KCl, 2 mM dithiothreitol (DTT), 5 mM MgCl₂, 5 mM imidazole, 10% glycerol, 0.1% NP-40, and complete EDTA-free protease inhibitor cocktail (Roche). The lysate was clarified at 10,000g for 60 min at 4°C. Subsequent purification steps were conducted on the ÄKTA Pure (GE Healthcare) system at 4°C.

The clarified lysate was loaded onto a 5-ml HisTrap FF Crude column (GE Healthcare), washed in a buffer containing 20 mM HEPES-KOH, pH 7.5, 100 mM KCl, 5% glycerol, 1 mM DTT, 5 mM MgCl₂, 0.1% NP-40, and 20 mM imidazole, and eluted with 75-ml linear gradient of 20 to 500 mM imidazole. The eIF2α containing fractions were then collected and applied to a MonoS HR 10/10 (GE Healthcare) equilibrated in a buffer containing 20 mM HEPES-KOH, pH 7.5, 100 mM KCl, 1 mM DTT, 5% glycerol, and 5 mM MgCl₂. The column was washed in the same buffer and eluted with a 75-mL linear gradient of 100 mM to 1 M KCl. eIF2α containing fractions were collected and concentrated with an Amicon Ultra-15 concentrator (EMD Millipore) with a 30,000-dalton molecular mass cutoff and chromatographed on a Superdex 75 10/300 GL (GE Healthcare) column equilibrated in a buffer containing 20 mM HEPES-KOH, pH 7.5, 100 mM KCl, 1 mM TCEP, 5 mM MgCl₂, and 5% glycerol. A typical preparation yielded approximately 2 mg of eIF2α from a 1-liter culture.

Purification of phosphorylated human eIF2α

eIF2α was expressed and purified as above, but with the following modifications: One Shot BL21 Star (DE3) *E. coli* were co-transformed with pAA007, pG-Tf2, and a third plasmid expressing the kinase domain of PERK (PERK 4: PERKKD-pGEX4T-1, Addgene plasmid #21817 donated by Dr. David Ron) and a resistance marker towards ampicillin. Transformed bacteria were grown in Luria broth containing ampicillin, kanamycin, and chloramphenicol. For purification, 1x PhosSTOP (Roche) was added to the lysis and purification buffers. Phosphorylation was confirmed by Phos-Tag SDS-PAGE (Wako) as described previously (30),

and by Western blot with an eIF2 α S51 phosphorylation-specific antibody (Cell Signaling, #9721).

Purification of tetrameric eIF2B($\beta\gamma\delta\epsilon$)

Tetrameric eIF2B($\beta\gamma\delta\epsilon$) and tetrameric eIF2B($\beta\gamma\delta\epsilon$) mutant proteins were purified using the same protocol as described for the decamer with the exception that expression strains were cotransformed without the eIF2B a subunit expressing plasmid. A typical preparation yielded approximately 0.75 mg of eIF2B($\beta\gamma\delta\epsilon$) from a 1-liter culture.

eIF2B($\beta\gamma\delta\epsilon$) tetramer with co-transformed plasmids: pJT073, pJT074

β N132D eIF2B($\beta\gamma\delta\epsilon$) tetramer with co-transformed plasmids: pAA012, pJT074

δ R250A eIF2B($\beta\gamma\delta\epsilon$) tetramer with co-transformed plasmids: pAA013, pJT074

δ R250E eIF2B($\beta\gamma\delta\epsilon$) tetramer with co-transformed plasmids: pAA014, pJT074

Cloning of mutant eIF2B expression plasmids

Mutant eIF2B constructs were generated by site-directed mutagenesis on pJT073 for β and δ , and pJT066 for α , using the primer indicated and its reverse complement.

β N132D (pAA012): 5'-

CCACTACGCTCAGCTGCAGTCTGACATCATCGAAGCTATCAACG-3'

δ R250A (pAA013): 5'-

CCCCGCCGAACGAAGAACTGTCTGCTGACCTGGTTAACAACTGAAACCG-3'

δ R250E (pAA014): 5'-

CCCCGCCGAACGAAGAACTGTCTGAGGACCTGGTTAACAACTGAAACCG-3'

EM sample preparation and data collection for ISRIB-bound eIF2•eIF2B and eIF2 α •eIF2B complexes

Decameric eIF2B($\alpha\beta\gamma\delta\epsilon$)₂ + eIF2($\alpha\beta\gamma$) + ISRIB: eIF2B($\alpha\beta\gamma\delta\epsilon$)₂ was diluted to 800 nM eIF2B, eIF2 to 2 μ M, and a stock solution of 200 μ M ISRIB in N-methyl-2-pyrrolidone (NMP) was added to a final ISRIB concentration of 2 μ M in a final solution containing 20 mM HEPES-KOH, pH 7.5, 100 mM KCl, 1 mM TCEP, 5 mM MgCl₂, 0.1% NMP, and incubated on ice for 10 min. An inter-amine bifunctional crosslinker (Pierce premium BS3, #PG82084) was then added at a concentration of 0.25mM, and the mixture was incubated on ice for 2 hours before quenching with 10mM Tris HCl.

Decameric eIF2B($\alpha\beta\gamma\delta\epsilon$)₂ + eIF2 α (P): eIF2B($\alpha\beta\gamma\delta\epsilon$)₂ was diluted to 800 nM and eIF2 α (P) to 2.4 μ M in a final solution containing 20 mM HEPES-KOH, pH 7.5, 100 mM KCl, 1 mM TCEP, 5 mM MgCl₂, 0.1% NMP, and incubated on ice for 10 min and cross-linked as described above.

Each sample was applied to Quantifoil R 1.2/1.3 200 or 400 Au mesh grids (Quantifoil, Germany). Quantifoil grids were used without glow discharging. Using a Vitrobot Mark IV at 4°C and 100% humidity with Whatman Filter Paper 1, 3.5 μ l of sample was applied to the grid, incubated for an additional 10s, then blotted with 0 mm offset for ~6 s and plunge-frozen in liquid ethane. Two data sets were collected. Both data sets were collected with on a 300 kV Titan Krios at UCSF using a K2 Summit detector operated in super-resolution mode; 3233 images for eIF2P•eIF2B and 3947 images for eIF2•eIF2B were collected at a magnification of 29,000 \times

(0.41 Å per super-resolution pixel, binned by a factor of 2 to 0.82 Å for subsequent processing). Dose-fractionated stacks were collected according to the parameters in Table S1.

Image analysis and 3D reconstruction

All dose-fractionated image stacks were corrected for motion artifacts, 2× binned in the Fourier domain, and dose-weighted using MotionCor2 (31), resulting in one dose-weighted and one unweighted integrated image per stack with pixel sizes of 0.822 Å. The parameters of the contrast transfer function (CTF) were estimated using GCTF-v1.06 (32) and the motion-corrected but unweighted images; automated particle picking was done using Gautomatch-v0.53 and averaged in 2D using Cryosparc v0.6.5 (33). For the 3D reconstruction, an ab initio reconstruction was done without symmetry, followed by homogeneous refinement. High-resolution homogeneous refinement was then performed in cryoSPARC, using dynamic masks and imposed C2 symmetry for 2 eIF2 bound to eIF2B, C1 symmetry was used for 1 eIF2 bound to eIF2B. These maps were low-pass filtered and sharpened in cryoSPARC. For eIF2α-phospho bound to eIF2B, manual refinement with C2 symmetry and automated sharpening were performed in cisTEM (34). Molecular graphics and analyses were performed with the UCSF Chimera package. UCSF Chimera is developed by the Resource for Biocomputing, Visualization, and Informatics and supported by NIGMS P41-GM103311 (35). Accession numbers for the structures are as follows: EMD-0649, EMD-0651, EMD-0664 (density maps; Electron Microscopy Data Bank).

Atomic modeling and validation

For all models, previously determined structures of the human eIF2B complex [PDB: 6CAJ (17)], human eIF2 alpha [PDBs: 1Q8K (20) and 1KL9 (21)], the C-terminal HEAT domain of eIF2B epsilon [PDB: 3JUI (26)], and mammalian eIF2 gamma [PDB: 5K0Y (36)] were used for initial atomic interpretation. The models were manually adjusted and rebuilt in *Coot* (37) and then refined in phenix.real_space_refine (38) using global minimization, morphing, secondary structure restraints, Ramachandran restraints, and local grid search. Then iterative cycles of manually rebuilding in *Coot* and phenix.real_space_refine with additionally B-factor refinement were performed. The final model statistics were tabulated using Molprobit (39) (Table S3). Map versus atomic model FSC plots were computed after masking using EMAN2 (40) and using calculated density maps from e2pdb2mrc.py with heteroatoms (ISRIB) and per-residue B-factor weighting. Solvent accessible surfaces and buried surface areas were calculated from the atomic models using UCSF Chimera. Final atomic models have been deposited at the PDB with the following accession codes: 1 eIF2•eIF2B•ISRIB (6O81); 2 eIF2•eIF2B•ISRIB (6O85); phosphorylated eIF2α•eIF2B (6O9Z). All structural figures were generated with UCSF Chimera (35) and BLENDER (<http://www.blender.org>).

GDP exchange assay

We modified the procedure to establish a loading assay for fluorescent GDP as described (1). Purified eIF2 (200 pmol) was incubated with a molar equivalent Bodipy-FL-GDP (Thermo Fisher Scientific) in assay buffer (20 mM HEPES, pH 7.5, 100 mM KCl, 5 mM MgCl₂, 1 mM TCEP, 0.1% NMP, and 1 mg/ml bovine serum albumin) to a volume of 18 μl in 384 square-well black-walled, clear-bottom polystyrene assay plates (Corning). The reaction was initiated by addition of 2 μl of buffer or purified wild-type and mutant eIF2B(βγδε) (2 pmol) under various conditions to compare nucleotide exchange rates. For comparison of tetramer or ISRIB-

assembled octamer, eIF2B($\beta\gamma\delta\epsilon$) (2 pmol) was preincubated in 0.1% NMP and 2 mM ISRIB for 15 min before 10-fold dilution into the final reaction. These concentrations of vehicle and ISRIB were used throughout unless otherwise specified. Fluorescence intensity for both loading and unloading assays was recorded every 10 seconds for 60 or 100 minutes using a TECAN M1000 Pro plate reader (excitation wavelength: 495 nm, bandwidth 5 nm, emission wavelength: 512 nm, bandwidth: 5 nm). Data collected were fit with a first-order exponential equation.

Negative Stain collection and 2D Classification

Decameric eIF2B($\alpha\beta\gamma\delta\epsilon$)₂ + eIF2($\alpha\beta\gamma$) + ISRIB: eIF2B($\alpha\beta\gamma\delta\epsilon$)₂ was diluted to 800 nM eIF2B, eIF2 to 2 μ M, and a stock solution of 200 μ M ISRIB in N-methyl-2-pyrrolidone (NMP) was added to a final ISRIB concentration of 2 μ M in a final solution containing 20 mM HEPES-KOH, pH 7.5, 100 mM KCl, 1 mM TCEP, 5 mM MgCl₂, 0.1% NMP, and incubated on ice for 10 min. EM grids of negatively stained sample were prepared by applying 4 μ L of sample to a 400 mesh copper grid covered with continuous carbon film and stained with 2 % (w/v) uranyl formate, following the established procedure (31). Negative-stain EM grids were imaged on a FEI Tecnai T20 microscope (Thermo Fisher Scientific, US) operated at 200kV and equipped with a TVIPS TemCam F816 (8K \times 8K) scintillator based CMOS camera (TVIPS, Germany). Images were recorded at a nominal magnification of 50,000 \times , corresponding to a pixel size of 1.57 \AA at specimen level, and with a defocus set to 1.2 μ m.

Fig. S1

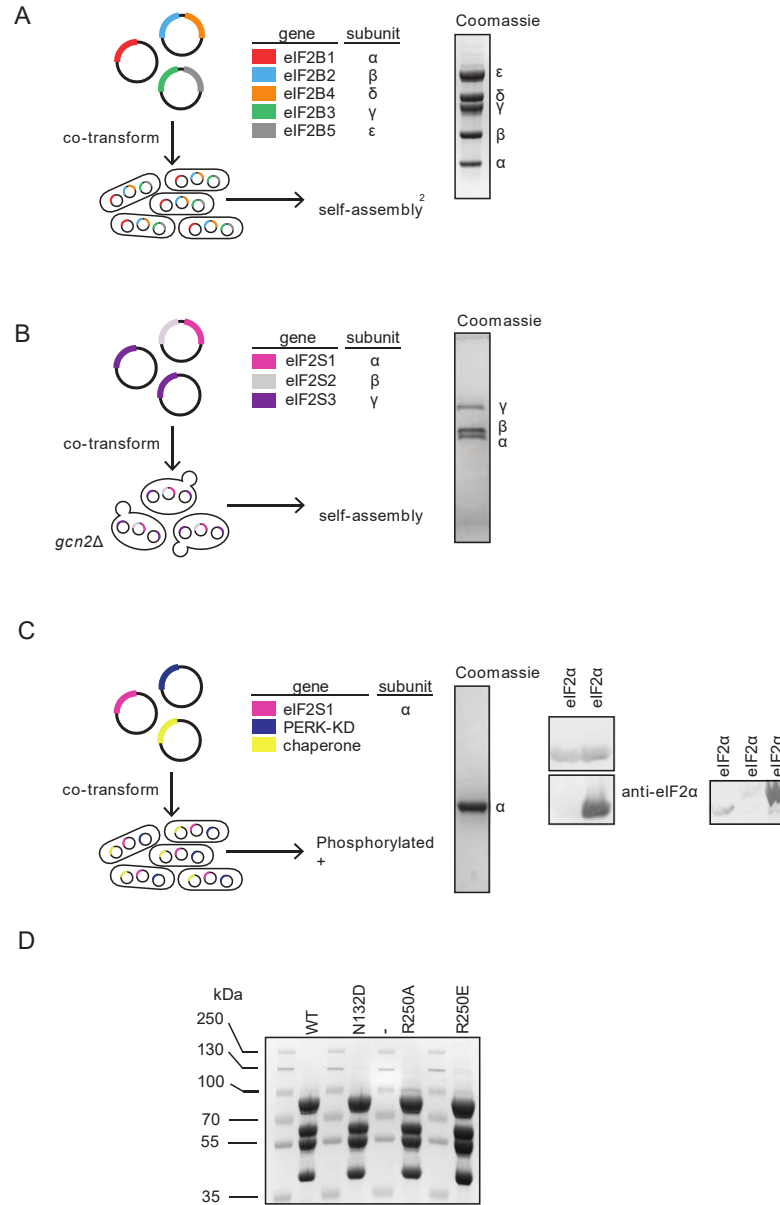


Fig. S1

Purification of eIF2, eIF2 α -P, eIF2B($\alpha\beta\gamma\delta\epsilon$)₂, and mutated eIF2B($\beta\gamma\delta\epsilon$) (A) Recombinant *E. coli* expression system and SDS-PAGE analysis for human eIF2B($\alpha\beta\gamma\delta\epsilon$)₂ as described in (20). (B) Recombinant *S. cerevisiae* expression system and SDS-PAGE analysis for human eIF2 as described in (22). (C) Recombinant expression *E. coli* system for phosphorylated eIF2 α and SDS-PAGE and Western blot analysis as described in (38). This expression protocol was

modified to include the chaperones GroEL, GroES and tig. (D) SDS-PAGE analysis of purified and mutated forms of eIF2B($\beta\gamma\delta\epsilon$).

Fig. S2

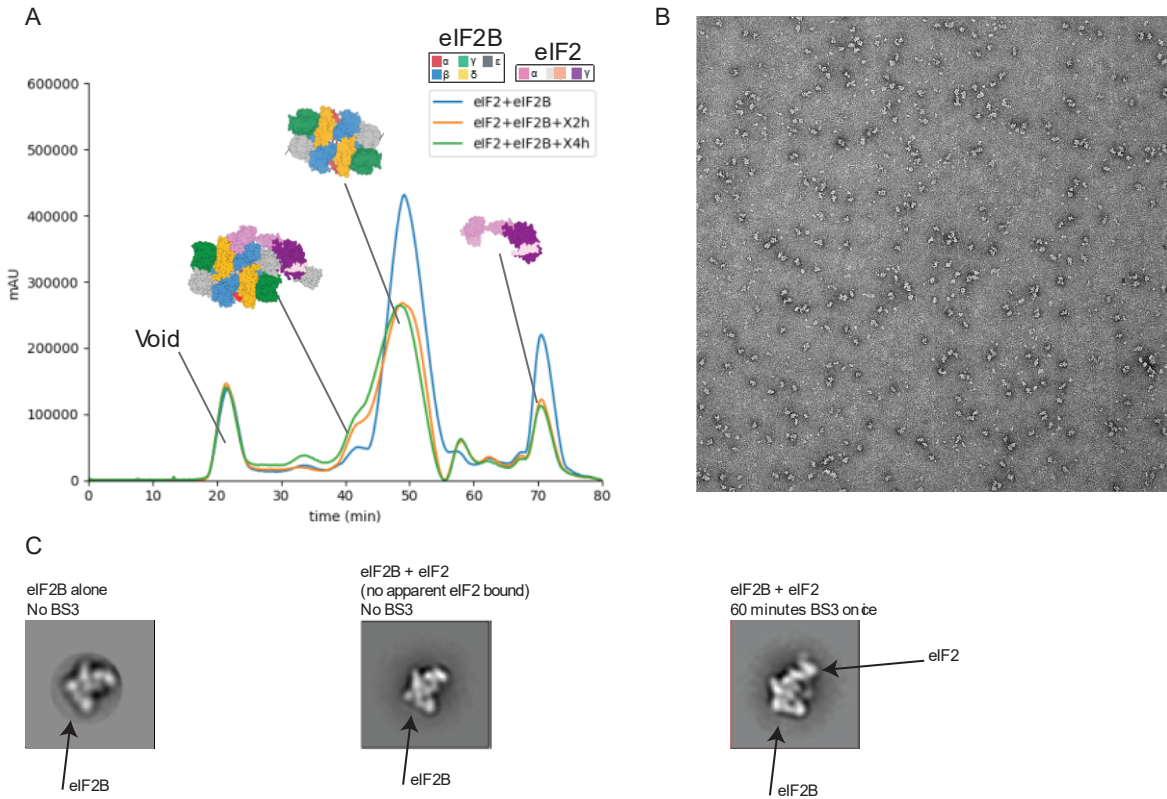
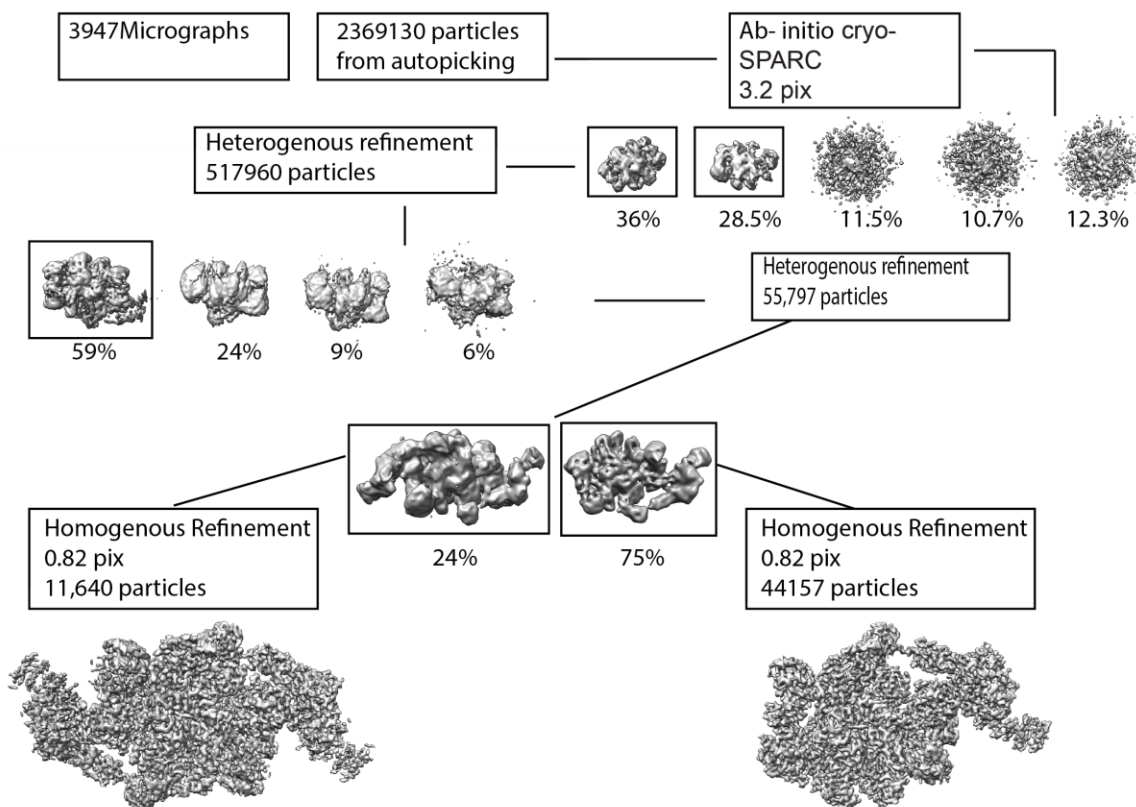


Fig. S2

eIF2 crosslinked to eIF2B. (A) Size exclusion chromatography (SEC) trace of eIF2 bound to eIF2B without crosslinker (blue), eIF2 bound to eIF2B incubated for 2 hours on ice with BS3 crosslinker (orange), and eIF2 bound to eIF2B incubated for 4 hours on ice with BS3 crosslinker (green). The void peak is comparable for each sample (blue, orange, and green). (B) Representative electron micrograph of negatively-stained eIF2•eIF2B incubated for 1 hour on ice with BS3 crosslinker. (C) 2D class averages of eIF2B alone (left), eIF2B incubated with eIF2 without cross-linking (middle), and eIF2 bound to eIF2B incubated for 1 hour on ice with BS3 crosslinker (right).

Fig. S3

A



B

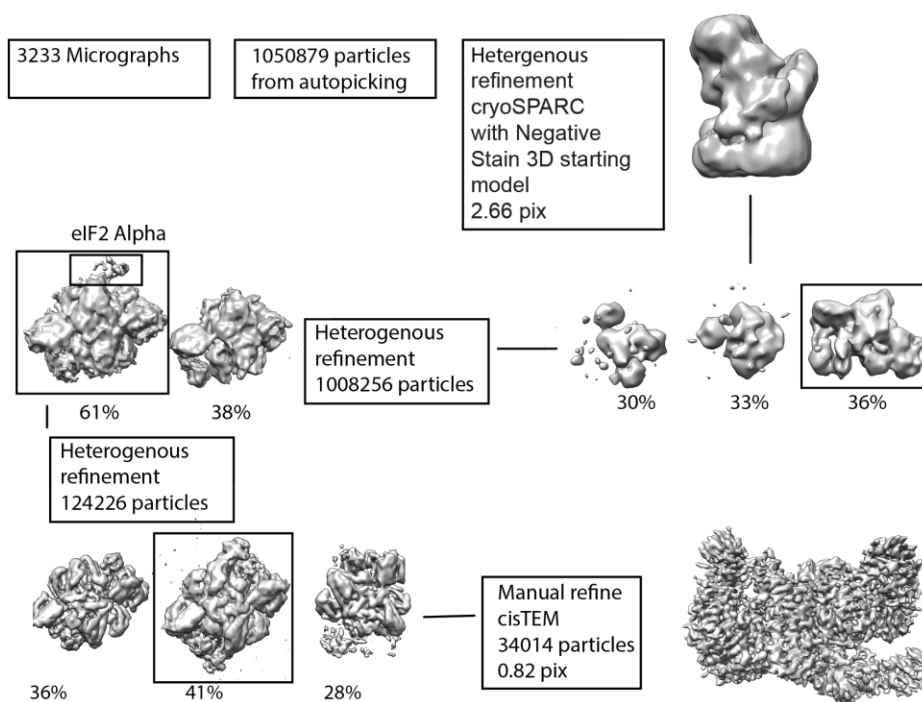


Fig. S3

Image acquisition and analysis workflow. Stages of preprocessing, image classification and refinement for (A) one eIF2 bound to eIF2B versus two copies of eIF2 bound to eIF2B; and (B) for eIF2 α -phospho bound to eIF2B.

Fig. S4

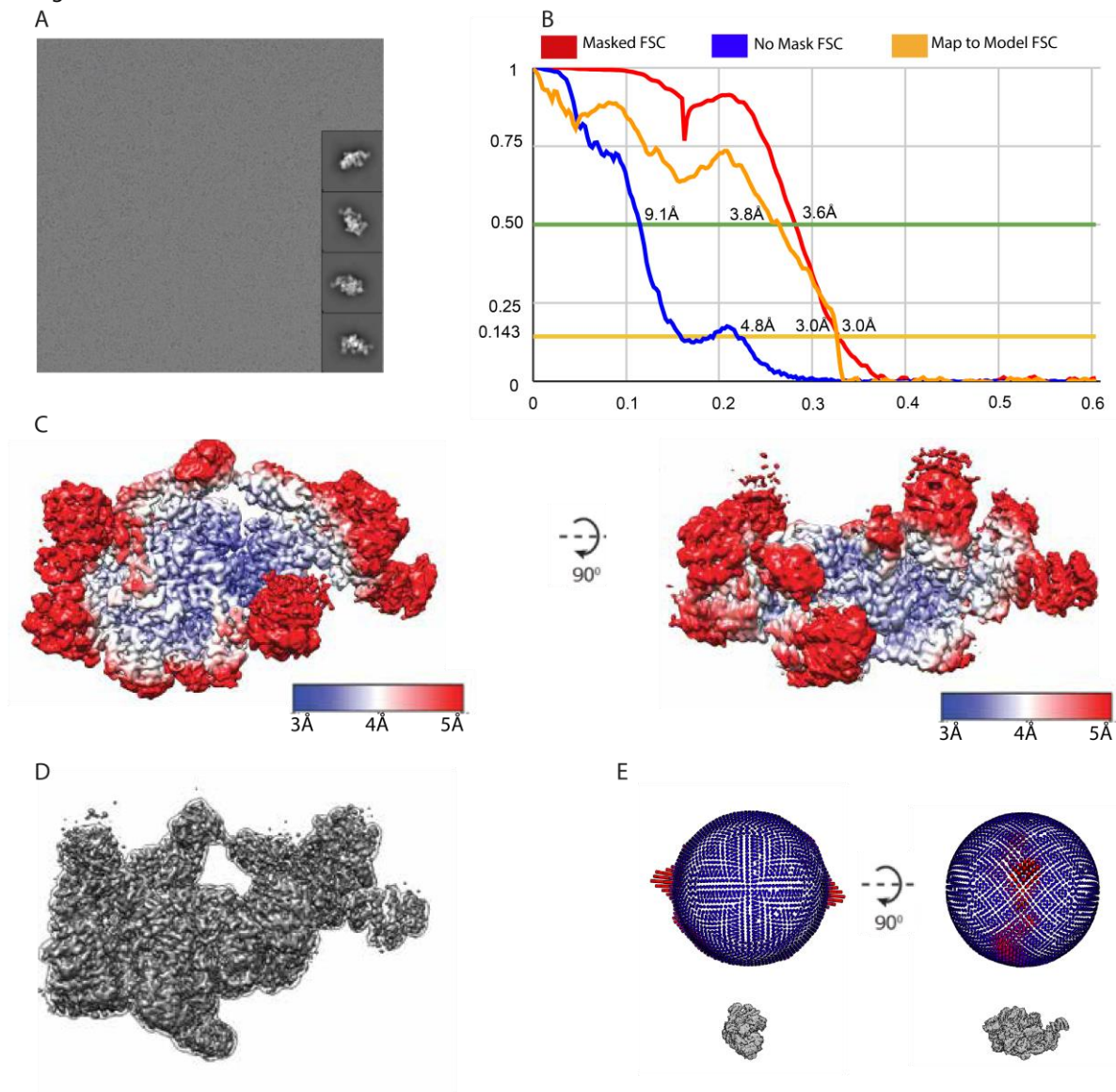


Fig. S4

Structure determination of one eIF2 heterotrimer bound to eIF2B. (A) A representative motion-corrected and dose weighted electron micrograph of frozen hydrated eIF2 bound to eIF2B, recorded as described in the Supplementary Materials and Methods. Inset, Representative 2D class averages calculated from selected particles. (B) FSC plots for the 3D reconstructions of eIF2 bound to eIF2B using a cryoSPARC-generated mask using automated procedures (red), eIF2 bound to eIF2B unmasked (blue), and eIF2 bound to eIF2B map versus atomic model (orange). (C) Local resolution estimates of eIF2 bound to eIF2B. The resolution is color coded as indicated by the scale bar. (D) 3D reconstructions of eIF2 bound to eIF2B docked within

boundaries of the mask generated within cryoSPARC. (E) Euler angle distributions of all particles used in the final 3D reconstruction.

Fig. S5

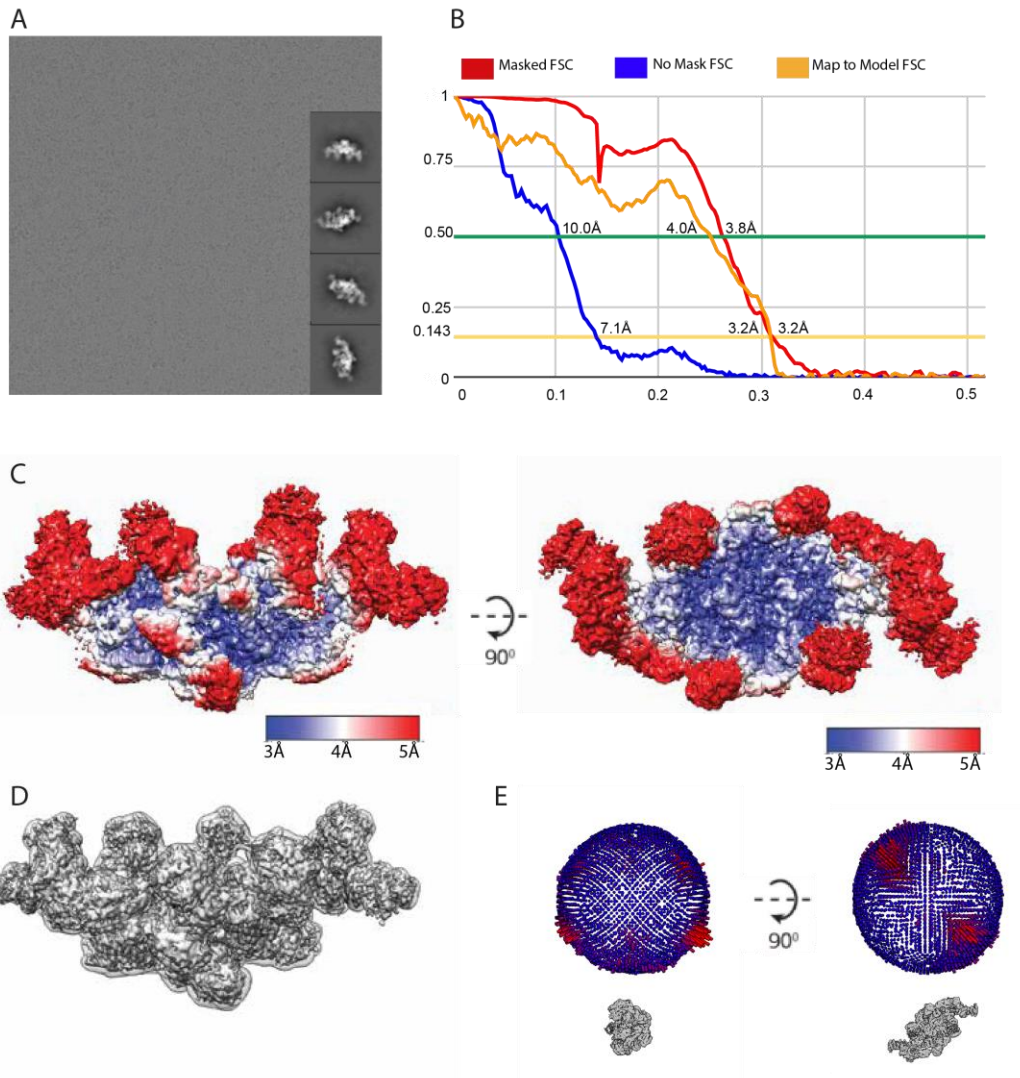


Fig. S5

Structure determination of two eIF2 heterotrimers bound to eIF2B. (A) A representative motion-corrected and dose weighted electron micrograph of frozen hydrated eIF2 bound to eIF2B, recorded as described in the Supplementary Materials and Methods. Inset, Representative 2D class averages calculated from selected particles. (B) FSC plots for the 3D reconstructions of eIF2 bound to eIF2B using a mask generated within cryoSPARC using automated procedures (red), eIF2 bound to eIF2B unmasked (blue), and eIF2 bound to eIF2B map versus atomic model (orange). (C) Local resolution estimates of eIF2 bound to eIF2B. The resolution is color coded as indicated by the scale bar. (D) 3D reconstructions of eIF2 bound to eIF2B docked within boundaries of the mask generated within cryoSPARC. (E) Euler angle distributions of all particles used in the final 3D reconstruction.

Fig. S6

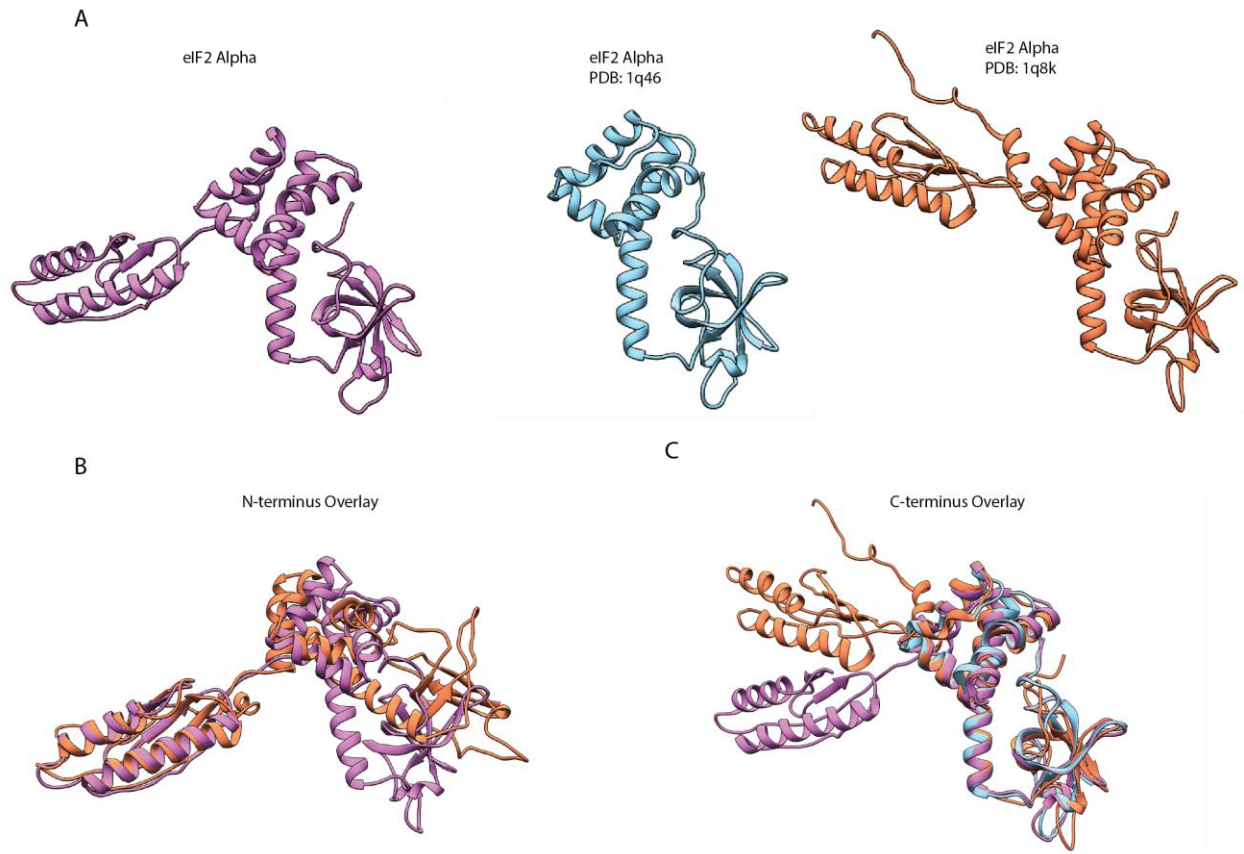


Fig. S6

Homologous eIF2 α structures used during model building. (A) eIF2 α atomic model (this study), eIF2 α crystal structure from *S. cerevisiae* (pdb:1q46)(20), eIF2 α solution structure from *H. sapiens* (pdb:1q8k)(21). (B) Structural alignment of the N-terminal domain of eIF2 α versus (C) structural alignment of the C-terminal domain of eIF2 α .

Fig. S7

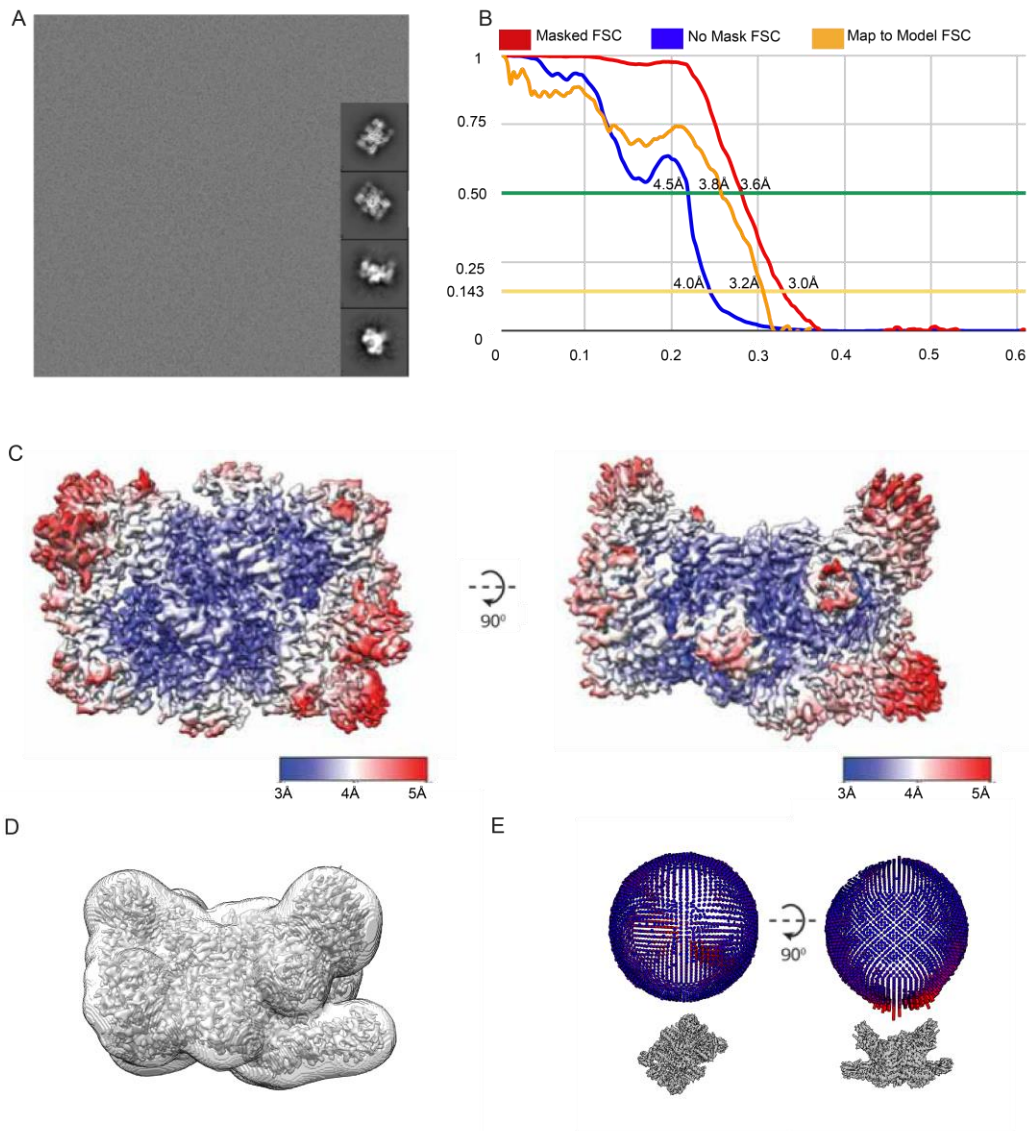
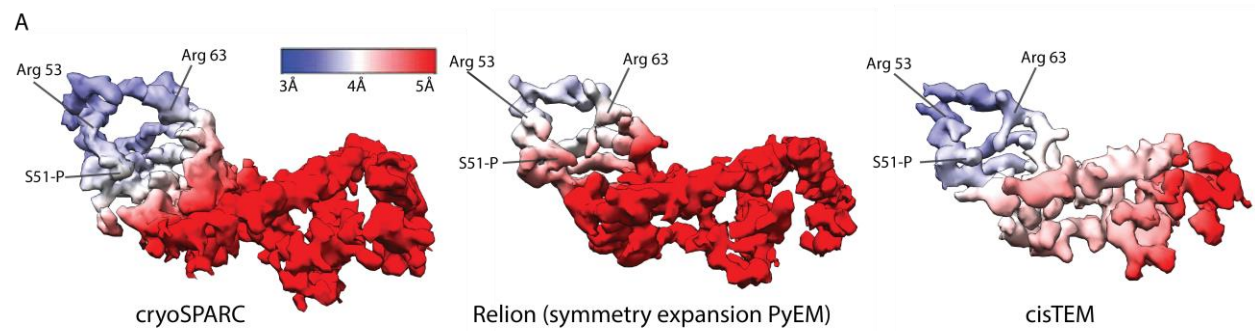


Fig. S7

Structure determination of two copies of eIF2 α -phospho bound to eIF2B. (A) A representative motion-corrected and dose weighted electron micrograph of frozen hydrated eIF2 α -phospho bound to eIF2B, recorded as described in the Supplementary Materials and Methods. Inset, Representative 2D class averages calculated from selected particles. (B) FSC plots for the 3D reconstructions of using a mask generated within cryoSPARC using automated procedures (red), eIF2 bound to eIF2B unmasked (blue), and eIF2 α -phospho bound to eIF2B map versus atomic model (orange). (C) Local resolution estimates of eIF2 α -phospho bound to eIF2B. The resolution is color coded as indicated by the scale bar. (D) 3D reconstructions of

eIF2 α -phospho bound to eIF2B docked within the boundaries of the mask used for FSC calculations. (E) Euler angle distributions of all particles used in the final 3D reconstruction.

Fig. S8



Local resolution estimates comparing the cryoEM density of eIF2 α -P refined with different software packages. (A) Segments of eIF2 α -phospho computed with cryoSPARC (left), versus RRELION with symmetry expansion as implemented within PyEM (middle, <https://github.com/asarnow/pyem>), versus cisTEM (right). Residues of the S-loop discussed in the main text are indicated and the nominal resolution is color coded as indicated by the bar.

	eIF2 α -phospho bound to eIF2B	eIF2 bound to eIF2B and two eIF2 bound to eIF2B
Pixel Size (Å)	0.822	0.822
Defocus Range	0.9 – 2.3	0.9 -3.0
Voltage (kV)	300	300
Magnification	29,000	29,000
Spherical Abberation (mm)	2.7	2.7
Detector	K2 Summit	K2 Summit
Detector Pixel Size	5	5
Per frame electron dose (e-/Å ²)	0.8	0.85
# of Frames	100	80
Frame Length (seconds)	0.1	0.1
Micrographs	3233	3947
Exposure (seconds)	10	8
Microscope	Titan Krios	Titan Krios

Table S1.

Data acquisition and image processing parameters.

	eIF2 Alpha P bound to eIF2B	eIF2 bound to eIF2B	Two eIF2 bound to eIF2B
Particles	34014	44157	11,640
Extracted particles	1050879	2369130	2369130
FSC Average Resolution, unmasked (Å)	4.1	6.3	3.32
FSC Average Resolution, masked (Å)	3.03	3.04	3.21
Map Sharpening B-factor	-78.7	-71.3	-60.4
Symmetry	C2	C1	C2
Final Reconstruction Package	cisTEM	cryoSPARC	cryoSPARC
Resolution Range	2.8-6.5	2.8-6	3.0-6

Table S2.
Refinement parameters.

	eIF2 Alpha P bound to eIF2B	eIF2 bound to eIF2B	Two eIF2 bound to eIF2B
Number of Atoms, macromolecules	25182	28549	33689
Number of Atoms, ligands	-	60	60
Molprobity Score	1.89	1.64	1.51
Molprobity percentile	81	91	94
Clashscore, all atoms	12.25	5.66	4.2
Clashscore percentile	62	91	94
RMS (bonds)	0.008	0.005	0.003
RMS (angles)	0.93	0.906	0.694
Ramachandran Favored (%)	95.78	95.29	95.58
Ramachandran Allowed (%)	4.22	4.71	4.42
Ramachandran Outliers (%)	0	0	0
Rotamer Outliers (%)	0.52	0.19	0.41
CaBLAM outliers (%)	1.91	2.5	2.75
B factors protein	111	74	108
B factors ligand	-	43	63
EMRinger score	2.74	1.77	1.99
Model Refinement Package (version)	phenix.real_space_refine (1.15rc3_3435)	phenix.real_space_refine (1.15rc3_3435)	phenix.real_space_refine (1.15rc3_3435)
Masked FSCaverage(Å)	3.0	3.0	3.2

Table S3.
Modeling statistics.

Movie S1.

Conformational morphing between the non-phosphorylated and S51-phosphorylated structures of eIF2 α , highlighting how phosphorylation leads to refolding of the S-loop.